scientific reports

Check for updates

OPEN

Augustus' solar meridian functioning and the birth of the western leap year

V. Baiocchi[1]✉, M. Baumgartner[2], M. Barbarella[3], M. T. D'Alessio[1], S. Del Pizzo[4], F. Giannone[5], F. Radicioni[6], A. Stoppini[6], G. Tosi[6], S. Troisi[4] & L. Alessandri[1]

In 12 BCE, Augustus undertook the responsibility for the calendar, which had gradually fallen out of alignment with the true dates of solstices and equinoxes. Augustus' calendar reform, entailing the introduction of a leap day every four years, coincided with the erection of a grand meridian in the Campus Martius, known in Latin as Horologium Augusti. This device utilized the obelisk of Psamtik II (6° century BCE) as its gnomon that casted its shadow upon a travertine floor inscribed with bronze reference marks. Despite the discovery of the obelisk in 18th century and partial excavation of the floor in 1980, comprehending its geometric intricacies, regarding both dimensions and positioning, remained a challenge due to the complexities of conducting precise geomatic measurements in subterranean environments. Consequently, uncertainties persisted regarding its operational mechanics, particularly regarding whether the marks denoted days or ecliptic degrees. This study presents accurate measurements and statistically rigorous analyses that enable a precise repositioning of the meridian and a careful reconstruction of its geometry. The results suggest that the marks likely denoted specific days of the year, as recalled by Pliny the Elder. This provides support to the hypothesis that the monument functioned as an empirical validation of Augustus' calendrical reform. In addition, the great accuracy achieved in positioning represents a fundamental aid in the desirable scenario to continue excavations of the meridian.

Keywords Augustus, Solar meridian, Ancient Rome, Leap year, Calendar, Least squares fit, Gnomon, Psamtik II obelisk

Since its initial discovery, the so-called *Horologium Augusti*, as described by Pliny the Elder in the 1st century CE[1] and partially excavated by E. Buchner in 1980 at Via di Campo Marzio 48 in Rome[2,3] (Fig. 1), has sparked extensive and intricate debates focused on reconstructing its original meaning, appearance and chronology[4–6]. Many authors have pointed out that the inauguration of the monument, which must have taken place after 10/9 BCE, occurred a few years after Augustus assumed the position of Pontifex Maximus in 12 BCE, and shortly before his decree (9/8 BCE) in which he corrected a calendrical error that had occurred during the pontificate of Marcus Aemilius Lepidus[7–9]. In fact, it was during Lepidus's tenure that the wrong practice of inserting leap days every three years instead of every four began.

Regarding its appearance, some scholars advocate for a genuine sundial, featuring the Egyptian obelisk from Heliopolis as the gnomon and an extraordinarily large marble pavement engraved with lines marking the days and hours[2,3,5,10–13]. Conversely, others contest this interpretation, suggesting instead a simple meridian, aligning with the sole pavement strip discovered by Buchner, oriented north-south[4,6,7,14–18]. Notably, despite numerous core samples and excavations, no evidence (if any, quite the contrary) has emerged to support the existence of a pavement extending east or west of the known one. Concerning its dating, there was long-standing speculation that the monument Buchner unearthed was not the Augustan one but rather a reconstruction from the Flavian era, commissioned under Domitian[2,3] or Vespasian[10] as the elevation also suggests. A recent coring conducted beneath the floor slabs has provided new data but unfortunately these are inconclusive as well[6,8] To sum up, the evidence does not provide a definitive basis for dating the monument and strongly supports the meridian hypothesis rather than a sundial. Nevertheless, certain aspects and specific technical details remain inadequately

[1]Sapienza University of Rome, Piazzale A.Moro, Rome 00185, Italy. [2]Soprintendenza speciale archeologia, belle arti e paesaggio di Roma, Piazza dei Cinquecento 67, Rome 00185, Italy. [3]University of Bologna, DICAM, Viale Risorgimento 2, Bologna 40136, Italy. [4]Parthenope University of Naples, Centro Direzionale Isola C4, Naples 80183, Italy. [5]Niccolò Cusano University, Via Don Carlo Gnocchi 3, Rome 00166, Italy. [6]University of Perugia, Via G. Duranti 93, Perugia 06125, Italy. ✉email: Valerio.baiocchi@uniroma1.it

Fig. 1. The meridian portion discovered during the archaeological excavations organized by DAI - Deutsches Archäologisches Institut.

understood. These encompass the very precise positioning of the pavement fragment found at approximately 7 m depth, the placement of the obelisk/gnomon base, its height, and lastly, the exact significance of the bronze notches that potentially indicate days or degrees.

Below, we will briefly present the current status of the four points of uncertainty that were just mentioned, and then provide a concise description of the approach we used to better estimate them.

As for the placement of the pavement fragment, upon its discovery, Ralf Bill[19], and Günter Leonhardt[6], members of the excavation team, initially situated the relief in relation to the current topography, independently creating two almost identical maps. Subsequently, two additional independent surveys were conducted. The first, led by Ismini Milaresis in 2013, utilized a metric wheel and compass; the second, led by Adalberto Ottati in 2014, employed a total station. A comparison between the two outcomes revealed an error in one of them due to the imprecise positioning of the roofs of the buildings within the meridian area, which formed the basis for anchoring to the modern situation. After identifying and rectifying this error, the two surveys aligned, and the result was published by Frischer in 2017 [6]. Unfortunately, the figure lacks absolute coordinates, and the lines depicting modern topography do not easily correlate with the existing structures.

The initial estimation of the obelisk base's location was proposed by Buchner before the discovery of the meridian pavement[20]. The scholar relied on the information provided by Stuart and De Marchis, contained in Bandini's book, both of whom observed, at least in part, the excavation of the obelisk[21], and the inscription still situated in Piazza del Parlamento 3, commemorating the finding of the obelisk base beneath the building. In 1980, the discovery of the meridian line, whose extension passes through the centre of the base, offered a precise constraint on the East-West axis. In 1995, Buchner organized a series of cores around that building in an attempt to intercept the base[11]. A partially edited report of this drilling campaign is available[6], along with the plan created by Leonhardt in May 1995, detailing the cores positions[5], and some cores, preserved at the Deutsches Archäologisches Institute and subsequently examined by G. Giordano and C. Rosa[6]. Regrettably, the numbering used by Leonhardt and the present numbering on the original cores do not align, making it possible to identify only few cores. Traces of tuff blocks, likely part of the monument's foundation, were found in four cores. Despite the lack of correlation with Leonhardt's numbering, it appears evident, as observed by Frischer[22], that these four cores should fall within those positioned by Leonhardt corresponding to the outline of the obelisk base on the 1995 plan, specifically those numbered from 10 to 14, otherwise, it would not be reasonable to hypothesize the base's location in that area. In the 1995 plan, Leonhardt proposes two outlines of the obelisk's base, with slightly different orientations. Depending on which one is correct, core 14 either intersects or does not intersect the base. It is worth noting that since only four cores exhibit traces of tuff, the correct solution should be the one that excludes core 14; otherwise, there would be five cores with tuff traces. This orientation corresponds to the one previously observed by Stuart, indicating a 15° tilt towards the west. In this case as well, the accuracy and precision of both survey and positioning of the cores are not known. Lastly, detailed information on the base dimensions and appearance is available from the reports of De Marchis and Stuart[21]; the latter also provides some accurate survey maps.

With regard to the height of the gnomon, it is important to emphasise that it is only partly related to the height of the obelisk, which forms only one of its components. The height of the gnomon that we have estimated is defined as the height of the shadow reference point, which consists of the perpendicular distance to the ground between the gnomon reference point (centre of the sphere? See supplementary Fig. S1) and the level of the floor intercepted by Buchner. So, in practice, the segments that need to be added together are: the radius of the sphere (a), a possible rod that connected the sphere to the top of the obelisk (b), the obelisk itself (c), its base down to its foundations (pedestal plus three plinths, d), and finally, the potential difference between the gnomon's ground level and the level of the meridian pavement at Via di Campo Marzio 48 (e). The measurement of (a) could be estimated, assuming that one of the globes preserved at the Capitoline Museums is that of Augustus' obelisk even if the association, although suggested by some authors, remains highly speculative[23].; the measurement (b) cannot be accurately calculated as no rod has ever been found; the heights of the obelisk (c) and its base (d) can be inferred, with some slight uncertainty, from the accounts of De Marchi and Stuart in Bandini (the height of the obelisk alone can also be measured again); the difference between the obelisk's ground level and the level of the meridian's pavement cannot currently be determined. Anyway our starting point rests on the description and measurements detailed by Stuart and De Marchis[21]. Stuart mentioned that the obelisk stood at a height of 71.4583 English feet, while its pedestal measured precisely one-fifth of the obelisk's height, amounting to 14.2916 feet. It should be noted that the decimal digits shown here are those provided in the original document by Stuart and are shown for completeness; in converting to metric, we will precautionarily stop at centimetres. Together, they totalled 85.7499 English feet, equivalent to 21.78 + 4.35 m = 26.14 m, using the conversion rate of 1 English foot to 304.8 mm[24]. This obelisk height value is very close to one of the most accredited values at present (21.79 m)[25]. According to Stuart and De Marchis, underneath the pedestal, there were two marble plinths and a travertine plinth, beneath which the foundation was located. According to Stuart, the travertine floor was positioned at the same level as the top of the travertine plinth. If we assume this as the base of the obelisk, we must therefore add to the height of the obelisk and its pedestal the two marble plinths, which were located at a higher level. Stuart's records indicate these measured 5 feet, 7 inches, and 60 centesimal (DN and EM in the text), approximately 1.71 m. Consequently, the total height of the obelisk and its base, excluding the sphere, reaches 27.85 m. If, on the other hand, we follow De Marchis's description, which places the travertine floor at the base of the travertine plinth, then we must also add the height of this plinth, 2 and 2/3 palm (0.59 m). In this case, the total height of the obelisk and its base reaches 28.44 m. Returning to gnomon height estimation, some authors have employed a simplified trigonometric approach since the height of the gnomon itself can be estimated from the length of the meridian. By extrapolating data from the sole section of the meridian discovered to date, Schütz proposed two heights: initially, 31.0 m[7], and later revising it to 30.70 m[15]. Albèri Auber, basing calculations on multiple assumptions, presented varying gnomon heights: 30.34 m; 30.505 m; 30.05 m[26], eventually settling

at 29.60 m[17]. It is worth noting that the measurement of 29.60 m had previously sparked interest as it equals 100 Roman feet. Albèri Auber suggests that this circumstance could have potentially eased the mathematical computations essential for the project's realization. Nevertheless, Schütz[27] takes an opposing view, highlighting that the calculations Albèri Auber refers to, reliant on a decimal system, would be anachronistic for the period. It is important to highlight that all these values have been calculated without a rigorous accuracy estimation.

The interpretation of the notches on the travertine floor is not unanimous. The majority of authors addressing this topic regard the notches as representations of days. However, Schütz[7,15,27] holds a different opinion, considering them expressions of the degrees of the ecliptic longitude: in this case, each notch would indicate an increase of 1 degree, totalling 181 notches. This interpretation stems mainly from the Greek inscriptions found on the floor, indicating the zodiacal signs of Aries and Taurus, on the west side of the meridian, and Leo and Virgo, on the east side. Since in the case of days, the number of notches in a leap year would have been 184 instead, and the total length of the meridian remains constant, the two hypotheses assume a different spacing between the notches. However, because that difference is minimal, up to now, it has not been possible to measure the distances between two adjacent notches with the necessary accuracy and consequently, understand what the correct hypothesis is.

To refine the definition of these four points, it was necessary to position the stretch of pavement, which includes the notches and inscriptions, with sub-centimetre accuracy, utilizing geodetic and geomatic techniques. Subsequently, by incorporating a reconstruction of the solar ray's inclination hitting the sundial, we estimated the relative geometry between the pavement and the gnomon, namely, the gnomon's height, the meridian's length, and the distance between the two sections of the monument. These quantities were associated with their respective standard deviation with which they are estimated.

Here we show that using an estimator, such as Least Squares method, on measurements taken with precise geomatic techniques, it is possible to extract the geometric information of the meridian with the accuracy allowed by the short stretch of pavement found so far. Simultaneously, statistically rigorous approaches make it possible to estimate not only the values of the unknowns but also their uncertainties. In this study, besides accurately positioning and reconstructing both the placement and the height (see following paragraph) of the gnomon with the same accuracy, we succeeded in estimating that the likelihood of the markings denoting days is higher than that of denoting degrees (see σd values in Table 1).

Results

An accurate survey was essential to obtain reliable results for determining the position and size of the gnomon and its distance from the meridian line. Surveys of the local network with GPS/GNSS receivers and the traverse with the total station provided the absolute position of the two sections of the monument with sub-centimetre accuracy with respect to an International Geodetic Reference System.

The mathematical relationship between unknown quantities and observations can be described through two mathematical formulations: referred to as Model 1/Topographic and Model 2/Pseudo-observations (Fig. 2) whose differences are explained in detail in the Methods paragraph. The redundancy of the number of measurements compared to the unknowns and the need to estimate the level of uncertainty with which they are calculated have required the use of statistical techniques based on the principle of Least Squares. A precise approach requires associating a 'weight' with observations derived from their precision levels.

In this contribution, we employ two categories of observations: geodetic measurements specifically carried out for this study and pseudo-zenithal observations ζ (as detailed in Eq. (3) of the methods section) which have been previously calculated and are accessible to the scientific community through NASA[28]. The geomatic measurements, made with laser scanner and photogrammetric surveys, yield a standard deviation value from the measurement process and subsequent analyses of 3–5 mm. Instead ζ values derive from considerations and corrections that reconstruct the sun position at the time the meridian was realised, and for this reason only assumptions can be made on their standard deviations. The results of the estimates performed under the

notch meaning: days				
Adjustment model	Model 1			Model 2
a	b	c	d	e
σd	0.005 m	0.005 m	0.005 m	0.005 m
σζ	0.001°	0.01°	0.1°	0.001°- 0.1°
H	31.171	31.148	31.138	31.154
σH	0.130	0.135	0.270	0.054
D_0	14.942	14.933	14.932	14.940
σD_0	0.062	0.066	0.147	0.030
a	0.144	0.150	0.307	0.062
b	0.0005	0.004	0.015	0.003
θ°	154.385°	154.129°	151.495°	150.612 -150.615°

Table 1. Estimation of the unknowns (H, D_0), their standard deviations (σH, σD_0), and the parameters of the error ellipse (a, B, θ°) for the year 4 BCE. Results obtained considering the hypothesis based on notches as day of year and both adjustment models (model 1: geomatic approach; model 2: pseudo-observations).

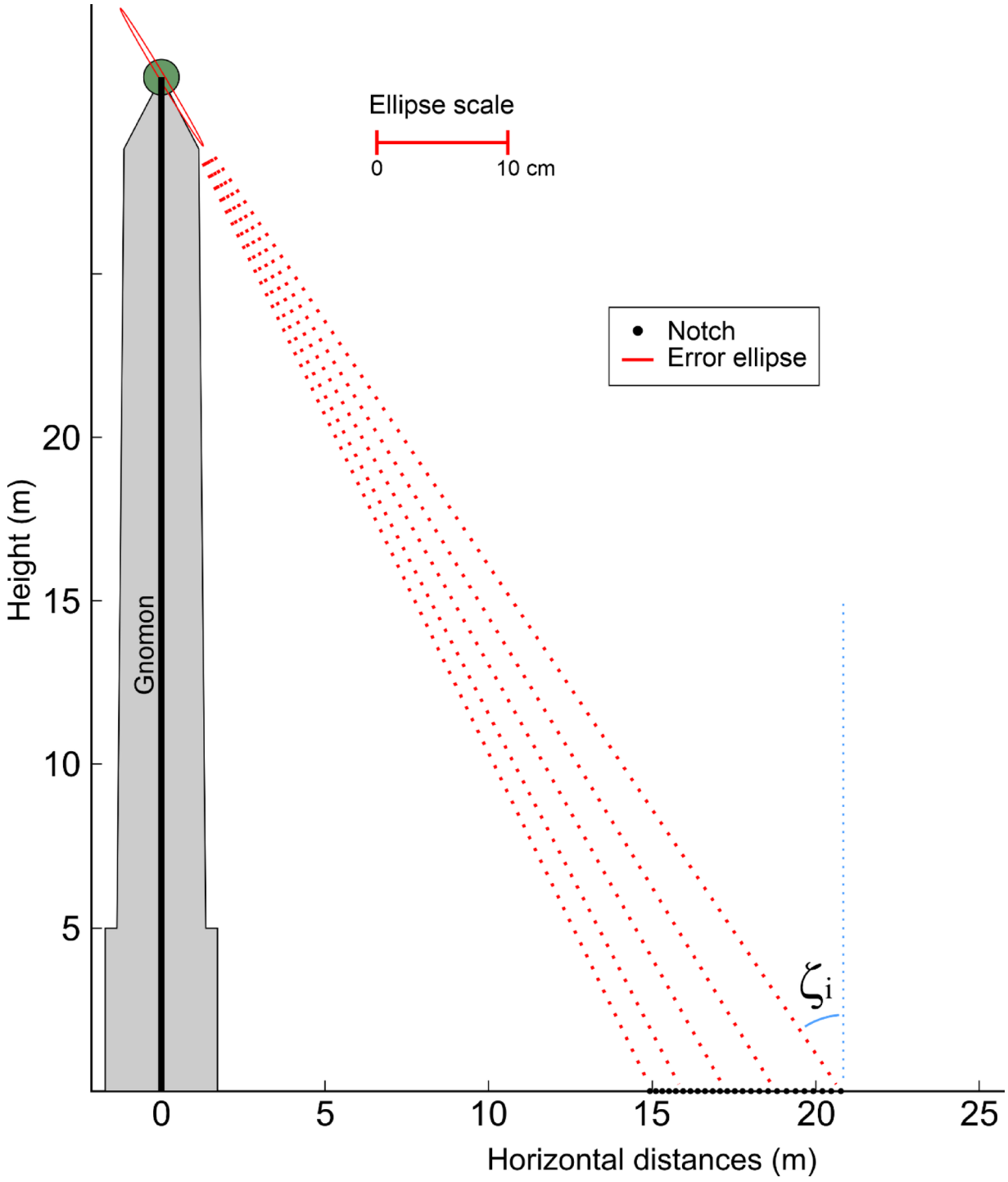

Fig. 2. Standard error ellipse for the position of the gnomon. Please note that the ellipse's scale exceeds that of the meridian.

different assumptions for σ_ζ will be presented below, while we refer to the methods section for the description of the procedures and definition of the estimated quantities.

Additionally, the analyses had to account for both hypotheses regarding the 'meaning' of notches whether they represent days of the year or degrees. As previously mentioned, in the two hypotheses, the number of notches would be different. More specifically, in the notches/degrees hypothesis, there is no difference between a leap year and a non-leap year. On the contrary, in the notches/days hypothesis, the number of notches can vary between the two semesters, and the position also changes depending on the year, returning to the same position at the end of a four-year cycle. Using the travertine floor as if it were at Augustus' level, in the following estimates, year 4 BCE will always be used in the calculations, because it is later than the construction of the obelisk and

because on the basis of specific analyses (see supplementary, Fig. S2) it presents a small deviation between the ζ-values in the two half-year periods. In any case, it has been assessed that, based on astronomical calculations, dating to the Flavian age does not result in significant variations.

Finally, the obtained results allowed us to determine the more probable hypothesis (days/degrees) and the measurements with higher likelihood.

Hypothesis based on notches as day of year

The values assumed for the uncertainties of d_i and ζ_i define the statistic model of observation useful for Least Squares adjustments: two computational models were employed, as we said, both based on the Least Squares criterion.

As regards the first adjustment model, the information required is the position of the gnomon in relation to the southern notch of the meridian line and the adopted statistical model; the coordinates of the top of the gnomon (unknown point) can be computed using a software developed for the "adjustment of planimetric networks" that provides the adjusted value of coordinates, their standard deviations, and the parameters of the standard error ellipses. In addition, the software allows an analysis of the standardized residuals. In Table 1, the two models with different values of standard deviation (SD) are compared for the same year (4 BCE). More in detail, columns b-d shows the solutions computed with different values of standard deviations of the angles $\boldsymbol{\zeta}$ (σ_ζ): height and distance of the gnomon together with their standard deviations (σ_H, σ_{D0}), and the parameters of standard error ellipse (a, b, θ°), major and minor semi-axes a and b, and orientation θ° are shown (the quantities are expressed in meters and degree).

The different values assumed for the standard deviation (σ_ζ ranging from 0.001 to 0.1 degrees) influences the unknowns H and D_0: the differences are 3 and 1 cm respectively. Respectively: H is the height of the gnomon while D_0 is the distance between the axis of the gnomon and the notch currently found further south. Conversely, their standard deviations change with the variation of the stochastic model: from 27 cm to 13 cm for H, from 15 cm to 6 cm for D. The solution used as a reference is: $\sigma_\zeta = 0.1°$, H = 1.138 m and $D_0 = 14.932$ m.

In the second adjustment model the unknowns are estimated considering for each notch the zenithal angle ζ_i and the distance from the first notch D_i, as described in detail in the methods section. The results obtained with this second model and the same choice of standard deviations on the measurements ($\sigma_d = 0.005$ m and $\sigma_\zeta = 0.001°$-0.1°) are shown in Table 1 (column e). In this second case, the different values of σ_ζ yield differences less than a millimetre, both in terms of numerical values or in terms of standard deviation and for this reason results are reported only one time (column e); this verification was repeated with more extreme values of σ_ζ to understand the variability of the estimations and the results of these further tests are reported in the supplementary (Tab. S1).

Figure 2 (where the height of the base of the pedestal aligned with the meridian plane should be considered merely schematic and not a geometric reconstruction hypothesis) shows the geometric configuration in the vertical plane of the gnomon, the notches on the meridian line and the ellipse of the standard error appropriately scaled.

The difference in the distance and height of the gnomon between the two models is 8 mm and 16 mm, respectively. The standard deviations for model 2 are smaller and amount 30 mm and 54 mm, respectively. The same reduction can be observed also for the parameters of the standard error ellipse. The two models therefore provide congruent results for the values of the estimates.

In conclusion, the results that we consider most reliable in the notch/days hypothesis are those calculated with model 2, namely: gnomon height, 31.154 m; distance from gnomon axis to southernmost notch currently visible, 14.940 m.; total track length (from summer solstice to winter solstice), 58.524 m.

Hypothesis based on notches as degrees of ecliptic longitude

The hypothesis based on the ecliptic longitude associated to each notch leads to different values for the sun declination, and therefore to different values for the zenithal angle in each notch of the meridian. Assigning to the obliquity of the ecliptic ε (inclination of the solar orbit on the equatorial plane) the value of 23.6964° calculated with Eq. (5) of the method section and varying the longitude of the ecliptic λ by an integer unit according to the relative value to be assigned to the notch of separation between the constellation of Leo and Virgo; the astronomical declination can be calculated as in Eq. (4) of the method section.

The same model (2/pseudo-observations) and the same choice for the standard deviation of distances and zenithal angles used for the previous assumptions (to $\sigma_d = 0.005$ m and $\sigma_\zeta = 0.1°$) leads to the results for the unknowns shown in Table 2.

As can be seen from the results reported in Table 2, the values of the distance and height of the gnomon, based on the assumption that the notches are associated with the degrees of ecliptic longitude, are smaller than

Adjustment model: 2 notches meaning: degrees of ecliptic longitude								
σd	σζ	H	σH	D_0	σD_0	a	b	θ°
0.005 m	0.1°	30.759	0.245	14.601	0.132	0.278	0.015	151.845°

Table 2. Estimation of the unknowns (H, D_0), their standard deviations (σH, σD_0), and the parameters of the error ellipse (a, B, θ°) for the year 4 B.C. Results obtained considering the hypothesis based on notches as degrees of ecliptic longitude and adjustment model 2 (pseudo-observations).

those reported in Table 1-column (e); on the other hand, the standard deviations of these values are considerably larger.

Considering that the notches spacing depends on the notches meaning (days or degrees of ecliptic longitude), the standard deviations analysis (model 2: $\sigma_H = 0.245$ and $\sigma_{D0} = 0.132$ notch meaning degrees; $\sigma_H = 0.054$ and $\sigma_{D0} = 0.03$ notch meaning days) shows a worse fit between model and data measured under the hypothesis of degrees.

In conclusion, the results that we consider most reliable in the notch/degrees of ecliptic longitude hypothesis are: gnomon height, 30.759 m; distance from gnomon axis to southernmost notch currently visible, 14.601 m; total track length (from summer solstice to winter solstice), 57.697 m.

3D modelling of augustus' Meridan

In this section we will attempt to reconstruct, on the basis of the results of our investigations and existing historical sources on the Meridian of Augustus, a three-dimensional georeferenced model of the meridian in which both the measured elements of the meridian and the obelisk are included, as well as the virtual modelling of the entire meridian and the original elements that are currently missing or replaced. As already mentioned, the obelisk was placed, after its rediscovery, in Monte Citorio Square, in a different position from the one it occupied at the time of its construction (Fig. 3a). For the construction of the three-dimensional model of the obelisk, a photogrammetric approach was applied using images taken with smartphone cameras. Numerous investigations into the performance of modern smartphone cameras compared to the digital cameras normally used in digital photogrammetry have shown that the results that can be obtained are very satisfactory[29].

The lenses of modern smartphones allow for excellent results in terms of image detail; the Structure from Motion algorithms implemented in digital photogrammetry software allow these images to be oriented and very high quality 3D models to be obtained[30].

In our case, 13 images with a resolution of 12 Mpx (4000 × 3000) of the obelisk taken by a smartphone, with an equivalent focal length of 26 mm, which photographed the obelisk from positions arranged in a circular sector of approximately 200° (it is not possible to photograph the obelisk from all directions, nor to take direct measurements on it, for security reasons), were used to create a 3D model of the gnomon actually located in Monte Citorio Square. All images were oriented using Agisoft Metashape 2.0.2[31], resulting in a reprojection error with an RMS (Root Mean Square) of 0.5 pixel. A dense point cloud was then extracted from the oriented camera network and it used to construct a polygonal mesh.

The resulting 3D model was further modeled in Blender 4.0[32] using a low-poly approach keeping the principal break lines in order to preserve sharp edges. The 3D model of the obelisk was positioned relatively to the surveyed meridian model in according to the calculation performed for hypothesis 1.

The reconstruction of the Augustus' meridian was carried out in Blender environment, collecting several models:

i. The portion of the meridian line surveyed by our team.
ii. The obelisk placed in Monte Citorio Square, surveyed by our team.
iii. The CAD model of the obelisk base as metrically described by De Marchis and Stuart[21].

Fig. 3. (**a**) The obelisk in its current position, representation extracted from one of the 13 images used for the construction of the 3D model and (**b**) the result of the complete modelling (Blender 4.0[32]).

iv. The CAD model of the sphere as represented on the central relief of the base of the Antoninus Pius column (see fig. S1 in supplementary).
v. The CAD model of the meridian dial, where the bronze meridian line was laid.
vi. The CAD model of seven steps where the obelisk base stands.

The first two 3D model (i & ii), as showed in Fig. 3b, were textured using real images acquired for performing the surveys as above described, such models were scaled with measurements collected in situ. The obelisk base was modeled in CAD environment, following the technical drawing and the measurements reported in De Marchis and Stuart[21], in Fig. 3b is represented in white color. Finally, all objects described in the literature, but whose measurements were not reported are modeled in gray; specifically: the sphere added to 3D model of the obelisk and the seven steps that support the obelisk base.

Discussion and conclusions

The Augustus meridian is a unique monument in terms of historical importance and scientific value; it consisted of a gnomon whose shadow was projected onto a bronze marking strip with orthogonal notches. The meridian probably served to demonstrate the correct choice of leap year every four years although there is no historical source to confirm this. In 1980, a travertine floor containing a short part of the meridian line was discovered.

The approach we employed started with a high-precision geomatic survey of its geometry, employing multiple surveying techniques to obtain accurate and high-precision results. This original approach made it possible to determine the position of the notches with an uncertainty of less than 3 mm.

To reconstruct the two fundamental quantities H and D_0, respectively height of the gnomon and distance of its axes from the southernmost notch of the discovered part of the meridian, we need to assign a specific angle value to each notch. This angle corresponds to the shadow cast by the gnomon on a particular date and was determined through astronomical calculations. Two assumptions were made: firstly, that each notch represented a day of the year, and secondly, that each notch corresponded to a degree of ecliptic longitude.

In this context, it's important to note that the data strongly indicates that the visible meridian pavement remains largely unaffected by significant displacements. This conclusion is drawn from the observation of the near-perfect horizontal alignment of the floor. Maintaining such precise horizontality would have been unlikely if there had been displacements or deformations, which typically exhibit a distinct differential component. Additionally, the slabs of the floor appear to be seamlessly fitted together, devoid of any gaps or displacements that would be indicative of deformations in the floor itself.

The data referring to 4 BCE were processed with two different computational models ('topographic' and 'pseudo-observations'), both based on the Least Squares criterion that provided basically the same estimates of the unknowns (D_0 and H) with differences of less than 2 cm between the two models. In the 'pseudo-observations' model, that resulted the most accurate, the uncertainties (in terms of standard deviation) associated with the estimated values are 3 and 5 cm for D_0 and H, respectively.

As mentioned above, two different hypotheses can be made about the function of the notches. Each of them can indicate a day or correspond to a 1° variation of the ecliptic longitude. While in a leap year the days are 366, the ecliptic degrees are 360 every year and therefore, over the distance of the entire meridian, the differences between the two hypotheses are small. However, they are not negligible considering the precision achieved in our measurements. The standard deviations obtained in the hypothesis notches/degrees is much less accurate, resulting in several tens of cm, while in the notches/days hypothesis the standard deviations are a few cm. It is concluded that the fit of the data is better under the notches/days hypothesis.

This contributes to strengthening two hypotheses. The first one is that the sundial represented a monumental materialization of Augustus's calendar reform, demonstrating the effectiveness of the corrections made. The second is that it also served the practical purpose of showing the passage of days, which could only be appreciated solely in relation to the large dimensions of the gnomon.

Extending the considerations from 9 to 1 BCE (Tab. S1) and thus with two leap years within it, the average of the values obtained for H and D_0 deviate by about one cm from the previous results reported in Table 1 for 4 BCE. The level of accuracy that is considered to have been achieved for the unknowns H, D_0 is of a few cm.

The present work has thus established the complete geometry of the instrument on the basis of all and only the currently visible elements. The estimations we have calculated under the various hypotheses deviate significantly from the values assumed by Auber[33] and are therefore not compatible with the 100 roman feet hypothesis if we consider (as Auber does) the Roman foot of 0.296 m, that is the most widespread and accepted estimate[34,35]. Schutz's[27] hypothesis, on the other hand, seems to fit better with our estimation under the assumption of notches as degrees of ecliptic.

It is useful to note that the Auber hypothesis of 100 feet would be much closer to the values estimated by Schutz and in this contribution if the Attic foot dimension (0.308 m)[34] was considered.

In conclusion, the results that we consider most reliable (notch/days hypothesis, model 2), are: gnomon height (height difference between the top of the gnomon and the discovered floor level), 31.15 m; distance from gnomon axis to the southernmost visible notch, 14.94 m; total track length (from summer solstice to winter solstice), 58.52 m.

This indicates that the obelisk casts a maximum shadow of 73.46 m (14.94 m + 58.52 m) on the ground at the winter solstice. This length lies well within the 80 m range that Hannah[12] empirically demonstrated to be a distance within which the shadow of a structure of such dimensions still remains distinctly visible.

Our estimate of the height of the gnomon can be compared with the data derived from Stuart (27.85 m) and De Marchis (28.44 m). The differences between these values range from 2.71 to 3.3 m and cannot be solely explained by the possible size of the globe. This supports the hypothesis of the existence, beneath the plinths,

of an additional base for which we have no measurement, but which could correspond to the "septem gradus circum" mentioned around 1500 by Pomponio Leto.

It should be noted that, since the differences between the astronomical values used in its construction during the Augustan period and those of the Flavian period are negligible, this new reconstruction does not provide additional data to support dating to either period. The "Domitianic" hypothesis primarily relies on the elevation at which the meridian was discovered, which appears to be higher than the level typically associated with the Augustan phase. However, it cannot be ruled out that the flooring of the sundial was originally designed to be elevated above the contemporary walking surface. Such a design choice would have been entirely logical, particularly given the area's susceptibility to frequent flooding by the Tiber River.

The data obtained from this study will also facilitate any further excavation of the surviving segments of the meridian, which, in all likelihood, still lie buried in this sector of the Campus Martius.

In addition, the accurate geometric reconstruction enabled a faithful and accurate virtual reconstruction that will be seen in a multimedia presentation available on Google Earth.

Methods

Why a geomatic survey was needed?

In order to verify certain hypotheses on the functioning of the meridian, historical studies must be accompanied by an in-depth knowledge of the geometry of the artefact and in particular the position of the notches in the only portion brought to light. As there is no comprehensive documentation on the subject, in-depth surveys were carried out using various techniques to verify the reliability of the results obtained.

The geomatic survey provides the absolute position of the meridian and the distances d_i between the 25 of the 28 available consecutive notches, while astronomical considerations allow each notch to be associated with a zenithal angle ζ_i (the angle between the observer's line of sight to the sun and the local vertical) to estimate both the height H of the gnomon and its horizontal distance D_0 to the first (southernmost) visible notch.

The geometry of the notches plays a key role and can be observed by performing accurate geomatic surveys on the find. Indeed, the different geomatic surveys techniques (Total Station, Terrestrial Laser Scanner, Digital Photogrammetry) have been used to obtain independent results whose congruence provides the level of reliability of the result achieved.

The number of observations is very redundant compared to that of the unknowns, so a Least Squares criterion can be adopted for the processing and this makes it possible to estimate the dimensions of the meridian much more accurately than with a simple trigonometric calculation that does not exploit all the measures taken. Further, the statistic approach allows for the value of the indeterminacy with which the unknowns are estimated, in terms of standard deviation.

Two different adjustment models can be adopted, the first of which invokes a *geomatic* approach (considering measurements of angles and distances among points) and the second directly considers the geometric relationship between observation and unknowns.

Geomatic survey

The surveying of the portion of the meridian floor, located in an underground cavity about 7 m below the current ground level, required the combined use of traditional geomatic techniques and satellite-based methods due to the complexity of the site and the surrounding urbanized area[36,37].

The survey has been georeferenced in the national Geodetic Frame ETRF2000/RDN2008 (EPSG:6708) by means of an external local GNSS network connected to some stations of the Lazio GNSS Permanent Network[38]. The underground room was then connected with a 3D traverse (Total Station measures) to the external GNSS network, and finally detailed surveys were carried out with total station, photogrammetry and laser scanning for an accurate and controlled description of the find.

GNSS network

In order to georeference the survey, a GNSS network was implemented outdoor, in the nearby "Piazza del Parlamento" (Parliament Square). This local network consists of 3 vertices, materialized by metallic markers. On the 3 points a measure session in static mode lasting about 4 h was performed with dual frequency GPS/GLONASS geodetic receivers.

The 3 local GNSS vertices were connected to 4 permanent stations of the GNSS network of the Lazio Region, whose coordinates are known with sub-centimetre accuracy thanks to the connection with the Italian geodetic reference network RDN[39]. The resulting 7 points network was post-processed using Topcon Tools 8.2.3[40].

Three different solutions have been computed:

- minimum constraint, connecting only the nearest permanent station (4 points network);
- minimum constraint, connecting all 4 permanent stations and assuming the nearest one as fixed (7 points network);
- all 4 permanent stations assumed as fixed (7 points network).

The three solutions have provided for the local GNSS vertices almost coincident coordinates values, with ±1–2 mm variations. The standard deviations of the coordinates are about 1 mm (horizontal) and 2 mm (vertical).

As for the altimetry, the GNSS solution has provided ellipsoidal heights, later converted into orthometric heights using the ITALGEO 2005 national geoid model[41].

Outdoor-indoor connection traverse

For the georeferencing of the underground room comprising the meridian artifacts, a three-dimensional local geodetic network (traverse) was established connecting the three outdoor GNSS vertices to the inner spaces. This part of the geodetic network was measured with a total station and prisms, replaced by opaque targets for the shortest traverse legs, where the prism target centres were not recognizable due to the high magnification of the instrument optic.

The traverse includes 10 vertices and spans from *Piazza del Parlamento* to the underground spaces, passing through *Via di Campo Marzio* and then along the building's interior corridors and stairs, until it reaches the room where a part of the meridian was discovered. The measurements were performed twice in both directions (forth and back). All total station measurements were repeated 3 times in straight position and 3 times in reverse. Forced centring devices were used for all points.

The network adjustment provided 95% confidence intervals of less than 1 cm in all directions.

Detailed survey of the meridian

The meridian remains, consisting of metal plates on the floor of the underground room, were measured by means of three different techniques, all supported by the network described above[37,43,44].

a) direct total station survey

From the last traverse vertex just above the meridian underground room, the points of intersection between the longitudinal south/north metal stripe and the transverse notches were directly measured by means of the total station (Fig. 4B).

For each intersection, 4 points were measured at the corners of the "cross" formed by the metal bands. The axis coordinates of the longitudinal band were then computed as the average of the east and west side points coordinates.

b) terrestrial laser scanner (TLS) survey

Following the traverse path from outside to the underground meridian room, 12 overlapping laser scans were performed. Applications of this technique to archaeological sites are described e.g. in Lerma et al.[45]. The laser scans were acquired with a FARO Focus 3D X130 phase difference scanner.

For the relative and absolute orientation of the scans, 21 squared checkerboard targets of 20×20 cm (the centres of which had been measured with the total station from the traverse vertices) and a set of six calibrated spheres of 145 mm diameter (only for relative orientation) were used. In this way, the TLS survey results were georeferenced in the same datum as the geodetic network.

The scans, processed with Cyclone 9.2.1[43], produced a three-dimensional model of the inner space including the visible part of the meridian. Figure 4A shows the overall point cloud of the 12 merged laser scans.

The intersection points between the longitudinal and transversal metal bands were newly measured on this 3D model, thus in an independent way from the total station measure described above. The coordinates obtained from this method result were almost coincident with those measured directly with the total station: the differences are within ± 1–2 mm.

c) photogrammetric survey

An accurate survey by digital photogrammetry was also carried out, obtaining a 3D model and an orthophoto (Fig. 4B) of the meridian floor independent from that derived by TLS. The relative and absolute orientation of the digital images was based on the same targets used for the TLS survey.

On the 3D model derived from photogrammetry the bands intersection coordinates were measured for a third time, obtaining values in agreement with the other two methods in a range of ± 1–2 mm.

The distances between the 25 consecutive notches were finally computed in order to proceed to an estimate of the gnomon height and its horizontal distance from the southernmost notch of the visible part of the meridian.

Although the formal standard deviations are of the order of 1–2 mm, taking into account the complexity of the survey we consider more appropriate to evaluate the distances uncertainty in the order of 3–5 mm. The local coordinates are in the Supplementary file (Tab. S2, paragraph 1.4).

Astronomic considerations

A meridian is a device whose task is to mark the time and day of the year using the sun's shadow cast by a gnomon on a flat surface. Projecting points of the celestial sphere from a point of view positioned in its centre is equivalent to build a gnomonic map. The projection of the path of the sun followed in the days of the solstices (parallels of declination) will be represented by two arcs of hyperbola; on the other hand, the projection of the celestial equator, a great circle that is the path of the sun in the two days of equinoxes, is a straight line (Fig. 5). The extreme marks of the whole meridian are touched by the gnomon shadow only once a year: at summer or winter solstice. Specifically, for a meridian located in the northern hemisphere at a latitude greater than the obliquity of the ecliptic, the gnomon casts its shadow on the southernmost sign on the day of the summer solstice and on the northernmost sign on the day of the winter solstice. In these two cases the sun reaches its maximum and minimum declination, respectively, as shown in Fig. 5. The other transverse marks on the meridian (such as that of Augustus) are generally used to indicate a day that falls between particular astronomical events (such as the day between an equinox and a solstice); they are touched by the sun's shadow twice a year, such as the equinox sign that is reached on equinox days when the sun's astronomical declination is zero.

Presumably, Augustus meridian was intended to show that the length of the year was 365 days and a quarter and, consequently, that the Julian calendar reform had been correctly applied by interposing a leap year of 366 days after three years of 365 days. After a period of 4 years, the sun would occupy the same position in the sky

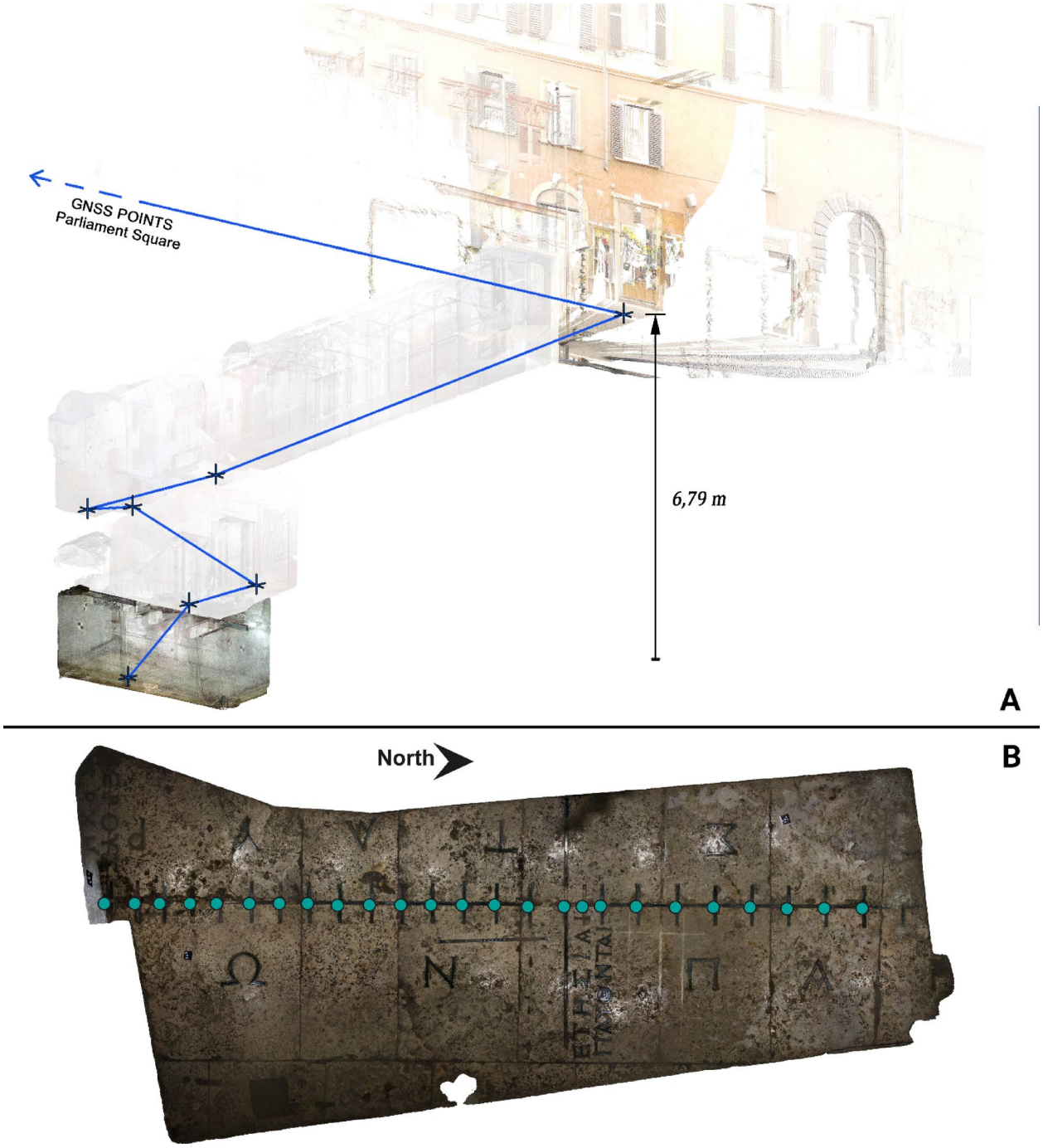

Fig. 4. (**A**) Overall point cloud of merged laser scans (Cyclone 9.2.1[42]); (**B**) Orthophoto of the ancient meridian with the measured notches highlighted.

and thus an obelisk of considerable height would cast its shadow on the same day on the signs of the identical day occupied 4 years earlier. The higher the obelisk, the more visible is the difference between the position of the shadow on the same day in different years. In astronomical terms, this implies that the declination of the sun when it crosses the meridian line is not exactly the same on the same day in two adjacent years, but has four-year cycles.

This trend is evident by calculating the astronomical declination of the sun at the passage of the Rome meridian on September 4th for each year from 9B.C. to 1B.C; the result steadily increases from 8.1° to 8.37° in the period 9BC-6BC, then decreases back to 8.09° in 5BC (leap year), the behaviour is repeated in the next four years obtaining 8.36° (2BC) and 8.08° in 1BC (leap year).

The same trend is followed by the zenithal angle ζ of the sun as well. Indeed, for a static observer it depends only on the astronomical declination δ (Eq. 1) because the latitude ϕ of the obelisk is constant:

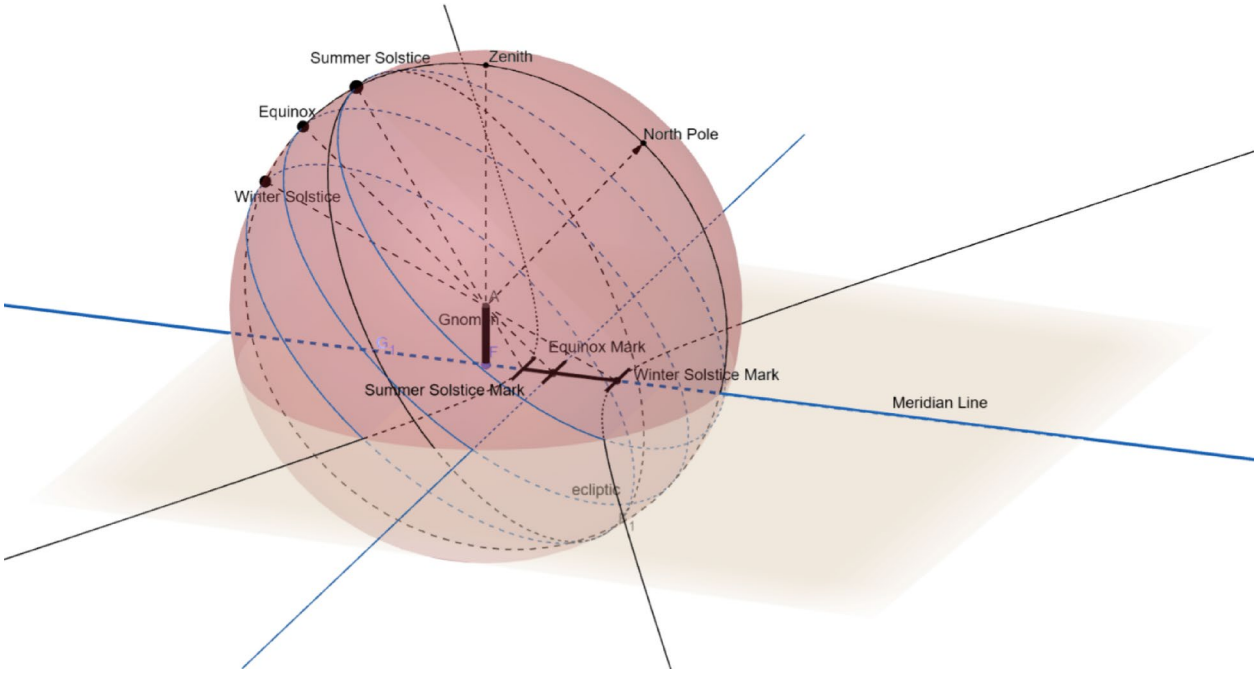

Fig. 5. Path of the sun and gnomon (GeoGebra 6.0.866.0[46]).

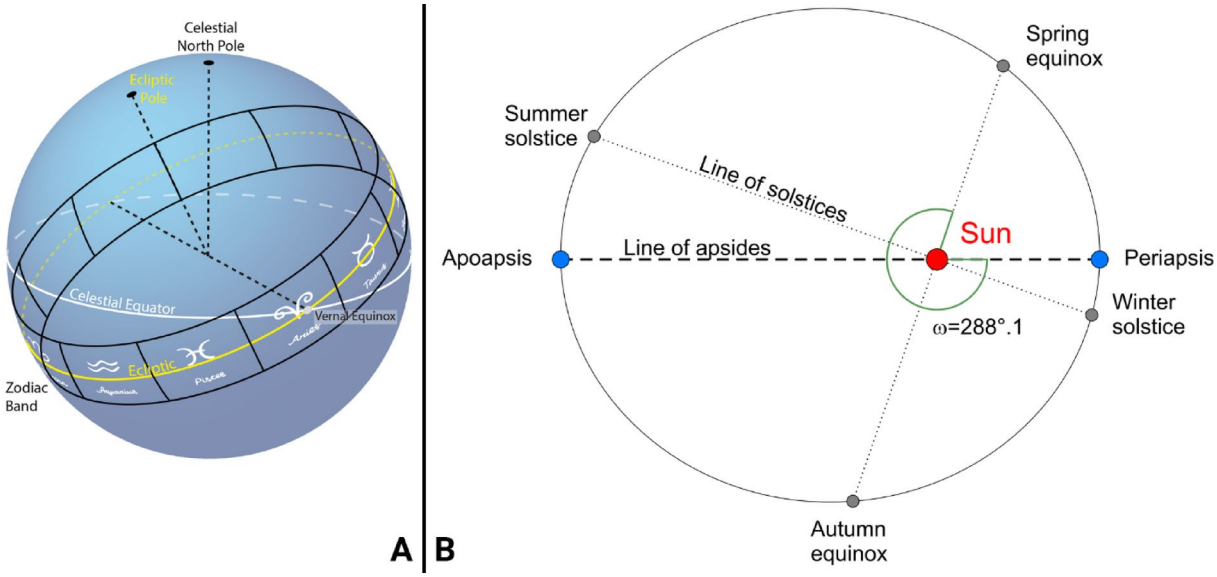

Fig. 6. (**A**) Apparent annual path of the sun and zodiac constellation; (**B**) Orbit of the Earth.

$$\zeta = \phi - \delta \tag{1}$$

In its apparent annual path on celestial sphere, the sun, following the ecliptic, appears projected onto the various zodiac constellations (Fig. 6A and B); on the line of Augustus meridian some signs with the names of the zodiac are engraved in bronze: in part, the inscriptions Krios (Aries), Tauros (Taurus), Leon (Leo), Parthenos (Virgo) and two meteorological-calendar phrases have been found, which have been recognized by Auber[17] as fragments of a "parapegma", a kind of calendar with meteorological indications inserted with respect to the constellations of the zodiac.

The two parapegmatic sentences can be translated as "The Etesii winds end" and "The summer begin". It is therefore possible to assign, with some approximation, a day of the year or degree and, consequently, the declination that will be indispensable for calculating the zenithal angle ζ associated with each notch.

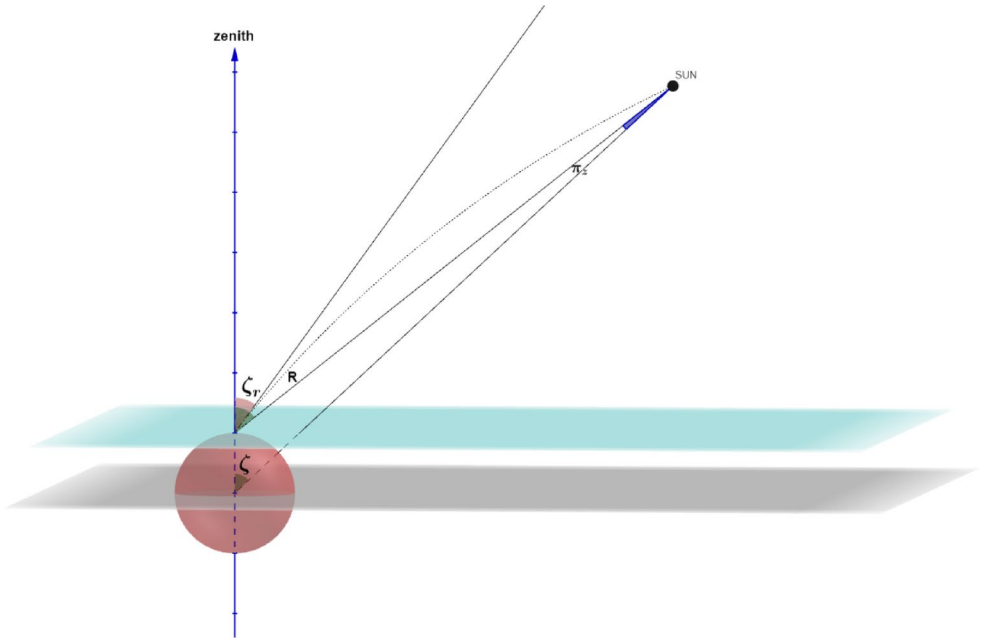

Fig. 7. Effect of diurnal parallax and atmospheric refraction on the computation of zenithal distance.

Auber[17] considered the 19th day before the autumn equinox as the day corresponding to the northernmost notch of the visible part of the meridian. In his work Auber uses a total of 28 notches, but only 25 notches can be identified from the orthophoto (Fig. 4A) by neglecting the two northernmost notches and the last southernmost notch. Consequently, the time reference becomes the 21st day before the autumnal equinox (or after the spring equinox) for the northernmost notch, hence the days corresponding with the 25 notches range from August 11 to September 4 (or from April 12 to May 6).

It is therefore necessary to know the exact day of the autumn equinox of about 2000 years ago. As a historical period, the year 4 BCE was chosen, a leap year near the time when Augustus built the meridian in Campo Marzio.

The sun's declinations, along with the instants of the equinoxes and solstices, have been estimated by using the Nasa Horizons tool[28].

Alternative hypothesis: days or degrees?

This analysis takes into account the hypothesis that many meridians of the past were constructed by matching each notch with a degree of ecliptic longitude of the sun. Therefore, each notch would correspond to 1° of ecliptic and the meridian would thus be divided into twelve sections, each one of 30°, i.e. the twelve constellations of the Zodiac. Starting from this assumption Auber used the Greek parapegma to reconstruct the meridian, including the missing part. In this case, the declination of the sun corresponding to each notch can be calculated using the following equation:

$$sin\delta \ = sin\lambda \, sin\epsilon \tag{2}$$

Where ε is the obliquity of the ecliptic, while λ represents the ecliptic longitude. In the hypothesis of Auber that the shadow of the sun falls on the northernmost mark on September 4th, there would be 21 days early until the autumn equinox (therefore almost 21° of ecliptic longitude).

According with the standard defined by IAU (International Astronomical Union), the value of the obliquity of the ecliptic changes slowly over the centuries and can be modelled by the following formula:

$$= 23^\circ \ 26' \, 21.448'' \ - \ 46.8150'' \, T \ - \ 0.00059'' \, T2 \ + \ 0.001813'' \, T3 \tag{3}$$

where T is the time measured in Julian centuries from the epoch J2000.0[49]; the average value of ecliptic obliquity computed for the year the Augustus meridian was built is 23.6964°.

Correction of the zenithal angles

Before using the algorithm for calculating the height of the gnomon, it is necessary to consider that the shadow cast by the gnomon on the meridian is influenced by the refraction suffered by the sun's rays passing through the atmosphere. Furthermore, the zenithal angle ζ must be calculated for an observer placed on the surface of the Earth (not in its centre), so the diurnal parallax π_z of the Sun (as shown in Fig. 7) must also be taken into account.

The parallax effect can be modelled by the following expression:

$$\pi_z = \frac{a\left(1 - s\sin^2\phi\right)}{d}\sin\zeta \tag{4}$$

where a and s represent the semi-major axis and the flattening of the reference ellipsoid, respectively, d the distance between the center of the Earth and the Sun.

For practical purposes, the reference ellipsoid can be replaced by a sphere and the distance to the sun can be considered constant. Since this correction, for the sun, does not exceed 8.8", we can use the following approximate formula to estimate the diurnal parallax expressed in seconds of arc:

$$\pi_z = 8.749'' \sin\zeta \tag{5}$$

Regarding atmospheric refraction R, there are several algorithms that can be used to model its effect as a function of the refracted zenithal angle ζ_r

$$\mathrm{R} = \mathrm{A}^*\tan\zeta_r - \mathrm{B}^*\tan^3\zeta_r \tag{6}$$

with R expressed in arc seconds, A = 60.39" and B = 0.07" and valid for $\zeta_r < 80°$ in normal atmospheric conditions (t = 0 ° and P = 760 mm). Bennett[48] suggests the following formula for computing the refraction

$$\mathrm{R} = \cot\left(\mathrm{h_r} + \frac{7.31^\circ}{\mathrm{h_r} + 4.4^\circ}\right) \tag{7}$$

as a function of the refracted elevation hr = 90°- ζ_r expressed in degrees and R expressed in minutes of arc. Sæmundsson[49] has instead developed a relationship in which refraction is calculated as a function of true elevation (h = 90°- ζ) and that is precisely the one to be used in our case:

$$\mathrm{R} = 1.02\cot\left(\mathrm{h} + \frac{10.3^\circ}{\mathrm{h} + 5.11^\circ}\right) \tag{8}$$

In the calculations to be carried out to obtain the height of the gnomon, the refracted zenithal angles ζ_r must be used because the apparent path of the sun's rays is examined, therefore the diurnal parallax and the refraction corrections must be subtracted from the zenithal angles ζ (Fig. 7).

Effect of the orbit's eccentricity

An argument of perihelion almost equal to 288° (Fig. 6B) produces a lack of coincidence between the line of the apsides and the line of solstices for the Earth's elliptical orbit around the Sun; according to Kepler's second law, it also generates both a different duration of the seasons and a different variation in the Sun's declination from the summer solstice. Therefore, the absolute value of the variation of the sun's declination in the months of increasing declination for a given number of days until the solstice has a different value if the same number of days is examined after the solstice. Similarly, the distance between the two extreme notches of the meridian remains that will be included in the calculation will refer to the change in declination that occurs in 25 days, but it will be different if this period is considered in the ascending or descending months, even if such period is symmetrical with respect to the solstice. This means that a meridian to be used as a calendar should have a double sequence of notches, one relating to the period of the ascending months (from the winter solstice to the summer solstice), the other for the descending months (from the summer solstice to winter solstice)[50]. The recovered part of the Augustus meridian shows only a sequence of notches, and so we need to understand whether this sequence is more appropriate for ascending or descending months. It is useful to point out that if the perihelion argument had a value equal to 270° there would have been a perfect coincidence of the notches for the ascending and descending months.

Estimation of height and gnomon distance by adjustment of measurements

The geomatic survey provides the absolute position of the meridian and the distances d_i between the 25 consecutive notches, while astronomical considerations allow each notch to be associated with a zenithal angle ζ_i (direction of the sun) to estimate both the height H of the gnomon and its horizontal distance D_0 to the first (southernmost) notch, Fig. 2. The number of observations is very redundant compared to that of the unknowns, so a Least Squares criterion can be adopted for the processing. Two different adjustment models can be adopted, the first of which invokes a *geomatic* approach (considering measurements of angles and distances among points) and the second directly considers the geometric relationship between observation and unknowns.

Geomatic approach. Adjustment model 1

In this approach the gnomon and the notches are considered points of a 'planimetric' network, connected by angles and distances, and the unknowns of interest (u) are the coordinates of the gnomon. Let us consider a local reference system with origin on the first (southernmost) notch of coordinates (0,0), the x-axis along the meridian and y-axis along the vertical. The centres of the notches and the gnomon are the points to be determined, belonging to the vertical plane passing through the obelisk and the visible part of the meridian. Hence the unknowns consist of the coordinates of the gnomon (x_G,y_G) and the x-coordinates of 24 notches, constrained on the x axis and therefore with y = 0, i.e. (x_i, 0).

The measurements considered in the adjustment consist of 24 distances d_i between successive notches and of 25 angles α_i with vertex on a notch and directions towards the gnomon and towards the adjacent notch (therefore along the x axis); these angles are easily computed from ζ_i.

For each observation we consider the equation that connects it to the unknowns (u) and introducing the residuals (v_i) we obtain a functional adjustment of indirect observations model:

$$A\,u = f + v \tag{9}$$

The observations are considered uncorrelated with equal standard deviation σ_d for all the distances and σ_α for all the angles, so the variance matrix results diagonal Σ_{ll}; the statistical adjustment model is $W = \sigma_o^{\,2}\,\Sigma_{ll}^{-1}$,

The random errors associated with angle measurements are not known with reliability and only hypotheses can be made about them.

The well-known solution for this model is[51]:

$$\hat{u} = \left(A^T W A\right)^{-1} A^T W f \tag{10}$$

$$\hat{\sigma}_0^2 = \left(v^T W v\right)/r\,\Sigma_{uu} = \hat{\sigma}_0^2 \left(A^T W A\right)^{-1} \tag{11}$$

Redundancy r is the difference between the number of measurements and the number of unknowns. Σ_{uu} is the Variance Covariance matrix of the estimates.

Pseudo observations adjustment model 2

We consider for each notch i the zenithal angle ζ_i and the distance from the first notch D_i. The functional relationship (non-linear in the unknowns) is:

$$H\tan\left(\zeta_i\right) = D_0 + D_i \tag{12}$$

Considering the pseudo-observation $T = \tan\zeta$, the relationship becomes:

$$HT_i = D_0 + D_i \tag{13}$$

This constraint must be valid for any pair of observations relating to each notch inserting the measured values $(\tilde{T}_i,\ \tilde{d}_i)$ and their corrections v_d and v_T; since the constraint relationship is non-linear in the unknowns, approximated initial values $\bar{h},\ \bar{d}_0$ and their corrections $\delta h,\ \delta d_0$ are considered for the unknowns *H* and *d*.

In matrix form the equation relating to the measures on the i-th notch results, neglecting 2nd order quantities, results:

$$\begin{bmatrix} -1 & \tilde{T}_i \end{bmatrix} \begin{bmatrix} \delta d_0 \\ \delta h \end{bmatrix} + \begin{bmatrix} \bar{h} & -1 \end{bmatrix} \begin{bmatrix} v_{T_i} \\ v_{d_i} \end{bmatrix} = \tilde{f}_i\,;\ \tilde{f}_i = \bar{d}_0 + \tilde{d}_i - \tilde{T}_i\,\bar{h} \tag{14}$$

The set of pairs of measures, for i = 1.2, … n, (where n is the number of notches) forms the following constraint model (whose rows are given by the previous formula):

$$A \begin{bmatrix} \delta d_0 \\ \delta h \end{bmatrix} + B \begin{bmatrix} v_{T_1} \\ \cdot \\ v_{T_n} \\ v_{d_1} \\ \cdot \\ v_{d_n} \end{bmatrix} = \tilde{f} \tag{15}$$

In this work a combined adjustment of observations and parameters is used:

$$A\,u + B\,v = \tilde{f} \tag{16}$$

As regards the stochastic model[52], indicating with σ_d the standard deviation associated with measures D and with σ_ζ those of declinations, by applying the variance-covariance propagation law to the pseudo-measures T_i can be obtained variances different for each i.

Each measure is considered uncorrelated from all the others, therefore the variance matrix of the observations Σ results:

$$\Sigma_T = \mathrm{diag}\left(\left(1 + T_i^2\right)^2 \sigma_\zeta^{\,2} \quad ;\ i = 1,2,\ldots n\right) \qquad \Sigma_d = \sigma_d^{\,2}\,I_n \tag{17}$$

$$\Sigma = \mathrm{diag}\left(\Sigma_T,\ \Sigma_d\right) = \mathrm{diag}(\sigma_{T_1}^{\,2},\ \sigma_{T_2}^{\,2},\ldots,\sigma_{T_n}^{\,2},\ \sigma_{d_1}^{\,2},\ \sigma_{d_2}^{\,2},\ldots,\ \sigma_{d_n}^{\,2}) \tag{18}$$

Defined the statistical model

$$W = \sigma_0^{\,2}\,\Sigma^{-1} \tag{19}$$

set

$$W_e = \left(B\, W^{-1} B^t\right)^{-1} \tag{20}$$

the solution is given by:

$$\widehat{u} = \left(A^t W_e A\right)^{-1} A^t\, W_e\ \ \widetilde{f} \tag{21}$$

and the variance matrix of the estimates is:

$$\widehat{\sigma}_0^{\,2} = \frac{\widehat{v}^t W \widehat{v}}{r}\, \Sigma_{uu} = \widehat{\sigma}_0^{\,2} \left(A^t W_e A\right)^{-1} \tag{22}$$

Data availability

The datasets used and analysed during the current study available from the corresponding author on reasonable request.

Received: 13 July 2024; Accepted: 29 April 2025
Published online: 12 May 2025

References

1. Pliny the elder. *Naturalis Historia*. vol. 36.71-73.
2. Buchner, E. Horologium solarium Augusti. Bericht Über die ausgrabungen 1979/80. *Mitteilungen Des. Deutschen Archäologischen Instituts Römische Abteilung*. **87**, 355–373 (1980).
3. Buchner, E. *Die Sonnenuhr Des Augustus*Mainz,. (1982).
4. Heslin, P. J. The augustus code: a response to L. Haselberger. *J. Roman Archaeol.* **24**, 74–77 (2011).
5. Haselberger, L. The 'horologium': where do we stand, and where should we go? *J. Roman Archaeol. Supplementary Ser.* **99**, 167–201 (2014).
6. Frischer, B. Edmund Buchner's solarium Augusti: new observations and simpirical studies. *Atti Della Pontificia Accad. Romana Di Archeologia Rend.* **LXXXIX**, 3–90 (2017).
7. Schütz, M. Zur Sonnenhur des augustus auf dem Marsfeld. *Gymnasium* **97**, 432–457 (1990).
8. Heslin, P. The Julian calendar and the solar meridian of Augustus: making Rome run on time. in The Cultural History of Augustan Rome: Texts, Monuments, and Topography (eds Loar, M. P., Murray, S. C. & Rebeggiani, S.) 45–79 (Cambridge University Press, Cambridge, doi:https://doi.org/10.1017/9781108635806.004. (2019).
9. Polverini, L. Augusto e Il controllo Del tempo. in Studi Su Augusto in Occasione Del XX Centenario Della Morte (eds Negri, G. & Valvo, A.) 95–114 (Giappichelli, Torino, (2016).
10. Buchner, E. Horologium Augusti. in Via Del Corso. Una Strada Lunga 2000 Anni (ed 'Onofrio, D.) 159–163 (Roma, (1999).
11. Buchner, E. Mainz,. Unter den Strassen und Kellern Roms, Sonnenuhr und Augustus- Mausoleum. in *Archäologische Entdeckungen. Die Forschungen des Deutschen Archäologischen Instituts im 20. Jahrhundert* 179–183 (2000).
12. Hannah, R. The horologium of augustus as a sundial. *J. Roman Archaeol.* **24**, 87–95 (2011).
13. Haselberger, L. A debate on the horologium of Augustus: controversy and clarifications. *J. Roman Archaeol.* **24**, 47–73 (2011).
14. Rodríguez-Almeida, E. Il Campo Marzio settentrionale: Solarium e Pomerium. *Atti della Pontificia Accademia Romana di Archeologia. Rendiconti* LI-LII 195–212 (1980). (1978–1980).
15. Schütz, M. The horologium on the campus Martius reconsidered. *J. Roman Archaeol.* **24**, 78–86 (2011).
16. Heslin, P. & Augustus Domitian and the So-Called horologium Augusti. *J. Roman Stud.* **97**, 1–20 (2007).
17. Albèri Auber, P. Reconstructing the Montecitorio obelisk of Augustus: a gnomonist's point of view. *J. Roman Archaeol. Supplementary Ser.* **99**, 63–76 (2014).
18. Frischer, B. & Fillwalk, J. New digital simulation studies on the obelisk, meridian, and Ara Pacis of augustus. *J. Roman Archaeol. Supplementary Ser.* **99**, 77–90 (2014).
19. Bill, R. Vermessungsarbeiten am horologium solarium Augusti. *Allgemeine Vermessungs-Nachrichten*. **90**, 147–154 (1983).
20. Buchner, E. Solarium Augusti und Ara Pacis. *Mitteilungen Des. Deutschen Archäologischen Instituts Römische Abteilung*. **83**, 319–365 (1976).
21. Bandini, A. M. *De Obelisco Caesaris Augusti E Campi Martii Ruderibus Nuper Eruto Commentarius* (Palearini, 1750).
22. Frischer, B. Edmund Buchner's solarium Augusti: new observations and simpirical studies. *Atti Della Pontificia Accad. Romana Di Archeologia Rend. LXXXIX*, 20–90 (2017).
23. Alföldy, G. The horologium of augustus and its model at Alexandria. *J. Roman Archaeol.* **24**, 96–98 (2011).
24. *The Britannica Guide To Numbers and Measurements*. (Britannica Educational Publishing, New York, (2011).
25. Zagari, F. Piazza Montecitorio: progetto di riqualificazione ambientale 1996–1998. *Camera dei deputati* (1998).
26. Albèri Auber, P. L'obelisco Di Augusto in Campo Marzio e La Sua linea Meridiana. Aggiornamenti e Proposte, in rendiconti Della pontificia accademia Romana Di archeologia. *Atti Della Pontificia Accad. Romana Di Archeologia Rend.* **84**, 447–580 (2012).
27. Schütz, M. Ancient and modern gnomonics: concerns and clarifications. *J. Roman Archaeol. Supplementary Ser.* **99**, 91–99 (2014).
28. Horizons System. NASA Jet Propulsion Laboratory, California institute of technology. (2023).
29. Andrews, J. et al. Validation of three-dimensional facial imaging captured with smartphone-based photogrammetry application in comparison to stereophotogrammetry system. *Heliyon* **9**, e15834 (2023).
30. Nocerino, E. et al. 3D reconstruction with a collaborative approach based on smartphones and a cloud-based server. *Int. Arch. Photogramm Remote Sens. Spat. Inf. Sci.* **XLII-2/W8**, 187–194 (2017). .
31. Agisoft. *Agisoft Metashape (Version 2.0.2)*. https://agisoft.com. Accessed 5 Mar (2025).
32. Blender Foundation. *Blender (Version 4.0)*. https://www.blender.org/. Accessed 5 mar 2025.
33. Albèri Auber, P. L'altezza dell'obelisco Di Augusto (in italian). *Atti Della Pontificia Accad. Romana Di Archeologia Rend. 2014–2015*. **87**, 451–472 (2015).
34. Jacono, L. Treccani enciclopedia italiana: Piede. *Treccani enciclopedia italiana* (2023).
35. Camporeale, S. Le unità di misura nella progettazione architettonica in Mauretania Tingitana. *Dialogues d'histoire ancienne* Supplément n°12, 79–100 (2014).
36. Baiocchi, V., Barbarella, M., D'Alessio, M. T., Lelo, K. & Troisi, S. The sundial of Augustus and its survey: unresolved issues and possible solutions. *Acta Geod. Geophys.* **51**, 527–540 (2016).

37. Baiocchi, V. et al. Integrated geomatic techniques for georeferencing and reconstructing the position of underground archaeological sites: the case study of the Augustus sundial (Rome). *Remote Sens.* **12**, 4064 (2020).
38. Regione Abruzzo. Informazione utenti rete GNSS – Regione Abruzzo. Collegio dei Geometri e dei Geometri Laureati della Provincia di Pescara. (2023).
39. Giorgini, E. et al. 15 Years of the Italian GNSS geodetic reference frame (RDN): preliminary analysis and considerations. in Geomatics for Green and Digital Transition (eds Borgogno-Mondino, E. & Zamperlin, P.) vol. 1651 3–14 (Springer International Publishing, Cham, (2022).
40. Topcon *Topcon Tools (Version 8.2.3)*. https://mytopcon.topconpositioning.com/it/support/products/topcon-tools (2025). Accessed 5 Mar 2005.
41. Barzaghi, R., Borghi, A., Carrion, D. & Sona, G. Refining the estimate of the Italian quasi-geoid. *Bollettino di Geodesia e Scienze Affini, Italian Military Geographic Institute (IGM)* LXVI no.3, (2007).
42. Leica Geosystems. *Cyclone (Version 9.2.1)*. https://leica-geosystems.com/-/media/files/leicageosystems/products/release%20notes/leicacyclone93rnen.ashx?la=pl-pl&hash=81FA34B2A9194B829DA0EEC97553E0B7. Accessed 5 Mar 2025.
43. Baiocchi, V. et al. Augusto's sundial: image-based modeling for reverse engineering purposes *Int. Arch. Photogramm Remote Sens. Spat. Inf. Sci.* **XLII–2/W3**, 63–69 (2017).
44. Baiocchi, V., Piccaro, C., Allegra, M., Giammarresi, V. & Vatore, F. Imaging Rover technology: characteristics, possibilities and possible improvements. *J. Phys. : Conf. Ser.* **1110**, 012008 (2018).
45. Lerma, J. L., Navarro, S., Cabrelles, M. & Villaverde, V. Terrestrial laser scanning and close range photogrammetry for 3D archaeological documentation: the upper palaeolithic cave of Parpalló as a case study. *J. Archaeol. Sci.* **37**, 499–507 (2010).
46. GeoGebra. *App GeoGebra (Ver. 6.0.876)*. https://www.geogebra.org/download?lang=en. Accessed 5 Mar 2025.
47. U.S, Naval & Observatory & H.M. Nautical almanac office. The astronomical almanac for the year 1990. *US Government (Printing Office)* B18 (1989).
48. Bennett, G. G. The calculation of astronomical refraction in marine navigation. *J. Navig.* **35**, 255–259 (1982).
49. Saemundsson, T. *Atmospheric Refraction \skytel* **72**, 70 (1986)
50. Fantoni, G. *Orologi Solari. Trattato Completo Di Gnomonica* (Technimedia Editore, 1988).
51. Mikhail, E. M. *Observations and Least Squares* (Univ. Pr. of America, 1982).
52. Ghilani, C. D. *Adjustment Computations: Spatial Data Analysis* (Wiley, 2017).

Acknowledgements

We would like to thank Claudia Valeri and Guy Devreux (Vatican Museum) for their assistance during the on-site examination of the Base of the Antoninus Pius column; Roberta Ialongo, Keti Lelo, Chiara Piccaro and Felicia Vatore for their assistance during the survey.

Author contributions

V.B., Mau. B., M.D., S.D., F.G., F.R., A.S., G.T., S.T. and L.A. contributed to the design and implementation of the research, M.D., Mar. B. and L.A. developed the historical, archaeological and museum research necessary for the correct historical reconstruction. All authors contributed to the analysis of the results and to the writing of the manuscript.

Declarations

Competing interests

The authors declare no competing interests.

Additional information

Supplementary Information The online version contains supplementary material available at https://doi.org/10.1038/s41598-025-00653-8.

Correspondence and requests for materials should be addressed to V.B.